Nonplanar Lifting Surface Problems by Means of High-Speed Digital Computers," *Journal of the Aerospace Sciences*, Vol. 28, Feb. 1961, p. 103–113.

[13] Lessing, H. C., Troutman, J. L., and Menees, G. P., "Experimental Determination of the Pressure Distribution on a Rectangular Wing Oscillating in the First Bending Mode for Mach Numbers from 0.24 to 1.30," TN D-344, Dec. 1960, NASA.

[14] Kolbe, C. D. and Boltz, F. W., "The Forces and Pressure Distribution at Subsonic Speeds on a Planar Wing Having 45° of Sweep Back, an Aspect Ratio of 3, and a Taper Ratio of 0.5," RM A51G31, Oct. 1951, NACA.

[15] Basu, B. C., "Aerodynamic Characteristics of Delta Type Wings with Curved Leading Edges at Subsonic Speeds," Rept. 26 396, F.M. 3529, Nov. 1964, Aeronautical Research Council.

[16] Bradley, R. G. and Miller, D. B., "Lifting Surface Theory—Advances and Applications," AIAA Paper 70-192, New York, 1970.

[17] Revell, J. D., "Comments on An Efficient Steady Subsonic Collocation Method for Solving Lifting Surface Problems," *Journal of Aircraft*, Vol. 8, No. 3, March, 1971, pp. 191.

[18] Cunningham, A. M., Jr., "Reply by Author to J. D. Revell," *Journal of Aircraft*, Vol. 8, No. 3, March 1971, pp. 192.

MARCH 1971 J. AIRCRAFT VOL. 8, NO. 3

Laminar, Transition, and Turbulent Boundary-Layer Characteristic with Favorable Pressure Gradient $M_1 = 9.6$

H. T. NAGAMATSU,* D. C. WISLER,† AND R. E. SHEER JR.‡
General Electric Research and Development Center, Schenectady, N. Y.

The effects of pressure gradient and roughness on the laminar boundary-layer transition and the characteristics of laminar, transition, and turbulent boundary layers were investigated in a hypersonic shock tunnel with a 4-ft long 10° cone. By maintaining a stagnation temperature of approximately 1400°K, the ratio of surface to stagnation temperature was 0.214, and the Mach number range over the heat gages was 7.8–10.2. Fast response platinum heat gages were used on the cone surface and the small wedge to detect the transition, the passage of turbulent bursts, and the local heat transfer rates. Boundary-layer surveys were conducted with impact pressure, total temperature, and wedge heat transfer probes to verify the existence of different types of boundary layers. From these measurements the characteristics of laminar, transition, and turbulent boundary layers were determined for a Mach number of 9.6. The experimental local heat transfer rates agreed reasonably well with the laminar theory and the turbulent theory which included both the density and velocity fluctuation terms.

Nomenclature

C_f = local skin-friction coefficient
C_h = local heat transfer coefficient
H_0 = freestream stagnation enthalpy
H_w = model wall enthalpy
l = Prandtl mixing length parameter
M = Mach number
P = pressure, psia
P'_o = freestream pitot pressure
P'_{o_4} = boundary-layer pitot pressure
q = local heat transfer rate, Btu/ft²-sec
Re_x = Reynolds number based on cone surface distance
Re_{δ^*} = Reynolds number based on displacement thickness
Re_θ = Reynolds number based on momentum thickness
T = temperature
u = local velocity
$\bar{u}$ = mean local velocity in turbulent boundary layer
x = distance along cone surface
y = distance normal to model wall
β = compressibility mixing length parameter
δ = local boundary-layer thickness
δ^* = displacement thickness
θ = momentum thickness
ρ = local density
$\bar{\rho}$ = mean local density in turbulent boundary layer
σ = Prandtl number
τ_w = local turbulent shear stress

Subscripts

0 = stagnation conditions
1 = local conditions outside boundary layer
5 = nozzle reservoir conditions

Received August 8, 1969; revision received April 8, 1971. This research was partially supported by the Ballistics Systems Division, United States Air Force.

* Research Associate. Associate Fellow AIAA.
† Aerospace Engineer; presently at the University of Colorado at Boulder, Colo. Associate Member AIAA.
‡ Fluid Mechanics Engineer. Member AIAA.

I. Introduction

THE knowledge regarding the laminar boundary-layer transition, local heat transfer rate, and skin friction for laminar and turbulent boundary layers at high Mach numbers is necessary for the design and development of advanced hypersonic vehicles, satellites, and space probes. Skin friction, ease of boundary-layer separation, and heat transfer rate depend upon whether the boundary layer is laminar or turbulent. There is a need for theoretical and experimental information on the effects of roughness, bluntness, pressure gradient, Mach number, real gas, wall cooling, and angle of attack on the transition Reynolds number at hypersonic Mach numbers. These effects have been investigated on 4- and 8-ft long 10° cones; some of the results are presented in Refs. 1–6.

At subsonic velocities, it was shown[7] that transition is a process involving the formation of turbulent spots, as postulated by Emmons.[8] This phenomenon is clearly visible in smoke tunnel photographs.[9] Turbulent bursts in the transition region were observed optically in the firing range[10,11] at supersonic speeds. Potter and Whitfield[12] investigated the

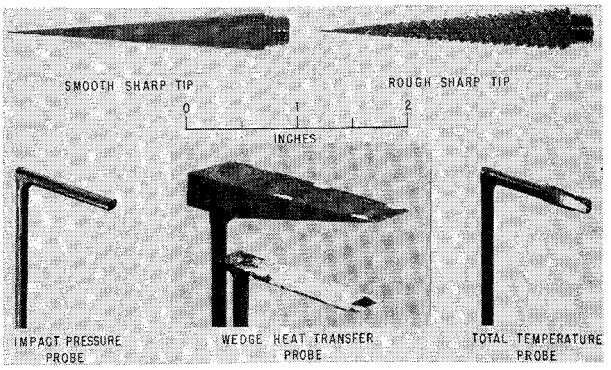

Fig. 1 Interchangeable tips and boundary-layer survey probes for 10° cone model.

laminar boundary layer on a hollow cylinder in a hypersonic wind tunnel. Nagamatsu et al.,[1–6] investigated the laminar boundary-layer transition on 4- and 8-ft cones[1–6] and the location of the critical layer.[13] The experimental evidence indicates that these turbulent bursts also occur at hypersonic Mach numbers.

The stability theories developed for low Mach numbers may not necessarily apply for high Mach number flows. For example, the theoretical work[14] predicts the experimental transition data[15] at Mach numbers of 1.6 and 2.2 but does not predict the experimental results[16] at a Mach number of 5.8. The three-dimensional nature of the boundary-layer instability was investigated analytically[17,18] and observed experimentally on a flat plate at low speeds.[19] The existing stability theories[20–24] agree with the experimental data for subsonic and slightly supersonic speeds,[15] but at a Mach number of 5.8, the experimental data[16] were completely different from the theoretical prediction.[24] Evidently for flow Mach numbers greater than approximately 3, the classical methods of solving the stability equation do not apply.[22]

The present investigation was undertaken to study the effects of tip roughness and favorable pressure gradient on surface heat transfer rate, laminar boundary-layer stability, and boundary-layer profiles on a 4-ft 10° cone.

II. Experimental Equipment

All of the tests were conducted in the straight through test section of the double nozzle hypersonic shock tunnel.[25] The 4-ft long 10° included angle cone model had a 50-μ in. surface finish. Surface roughness was generated by cutting multiple right- and left-hand threads on the 2.25-in. long stainless steel tip, so that the roughness fell below the effective cone surface.

Static pressure was measured along the cone surface using lead-zirconate-titanate pressure transducers. Standard Kistler Model 401 quartz gages were used to measure free stream impact and nozzle reservoir pressure. Thin film sputtered platinum surface heat transfer gages[26] were located at 180° from the pressure gages. At 34.5 in. from the cone tip, the boundary layer was surveyed vertically with three types of probes: a slightly flattened impact pressure probe with an outside diameter of 0.100 in. and a wall thickness of 0.005 in., a small total temperature probe with an unbonded strip of 0.0005-in. thick platinum mounted at the stagnation region, and two sizes of wedge heat transfer probes.[4] Both of the wedge probes had a thin film heat transfer gage sputtered on the top surface. A photograph of the probes is presented in Fig. 1, and additional information about the shock tunnel and associated instrumentation is presented in Refs. 1–6.

All of the instrumentation for the cone model was dynamically calibrated in an 8-in.-diam calibration shock tube over the pressure and temperature ranges expected through the boundary layer and on the cone surface.

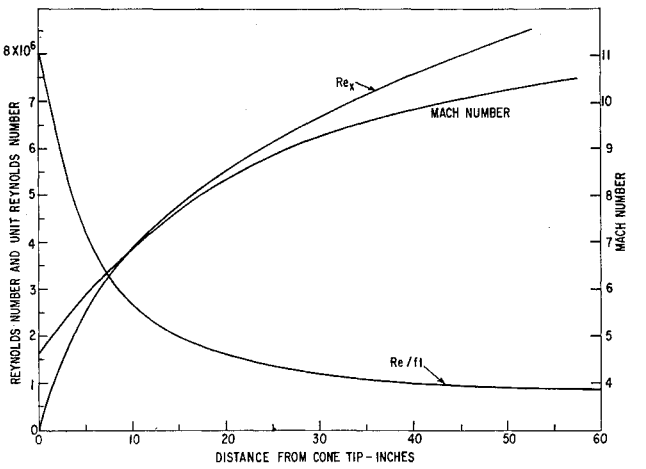

Fig. 2 Mach number, unit *Re* and *Re* distribution for reservoir pressure $P_5 \approx$ 1245 psia and temperature $T_5 \approx$ 1400°K.

III. Experimental Procedure and Results

The reservoir conditions behind the reflected shock were controlled by the initial temperature and pressure in the driven tube and the strength of the incident shock. All of the tests were conducted at a stagnation temperature of approximately 1400°K. This produced a model wall temperature to stagnation temperature ratio of 0.214. The expansion process in the nozzle was investigated by measuring the static and impact pressure along the axis of the nozzle. The reservoir pressures were high enough to have nearly equilibrium expansion. Mach number, pressure, density, temperature and velocity variations along the axis of the nozzle were calculated using the equilibrium thermodynamic data for air.[27]

The cone surface pressure showed a smooth variation with simply a finite increase over the empty nozzle case. This indicated that no significant disturbances were introduced into the nozzle flow by the presence of the model. It also indicated that the flow outside the nozzle exit was expanding as a freejet, probably due to the low initial dump tank pressure. The ratio of the test section impact pressure to reservoir pressure remained fairly constant once the nozzle flow was established.

Source-type flow over the conical model produced a fairly large increasing Mach number gradient and a decreasing pressure gradient along the cone surface. For a hypersonic source flow, the local temperature, hence the local speed of sound, decreases as the Mach number increases such that the local velocity remains almost constant. The velocity gradient was 2.7 fps/in. Weil[28] has calculated the effects of velocity and pressure gradients on compressible flow, based upon the theory of Lin and Lees,[22] and found that they are negligible for a freestream Mach number of 4.

The variation of Re/ft and Re_x is presented in Fig. 2. The unit Reynolds number Re/ft was calculated using the local properties just outside the boundary layer as determined from the measured cone surface pressure (Fig. 3) and the reservoir conditions. The surface Reynolds number Re_x for any given point was determined by integrating the Re/ft curve up to that surface location. A more detailed discussion of the significance of integrated Reynolds number is given in Refs. 4–6.

IV. Discussion of Results

A. Breakdown Mechanism of Hypersonic Laminar Boundary Layer

In the earlier references,[1–6] it was observed that transition begins with the appearance of turbulent bursts. It seems as if locally the laminar boundary layer breaks down with a corresponding sudden change in pressure, temperature, and heat

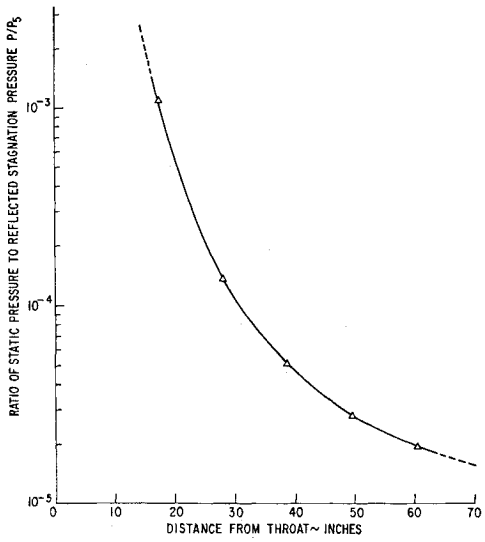

Fig. 3 Static pressure distribution for 10° cone in hypersonic nozzle, $T_5 \approx 1400°K$.

transfer. In the early stages of transition, these bursts do not occur frequently, and most of the time at a given location the boundary layer is laminar. As the Re increases, the magnitude of these turbulent bursts become larger,[1-6] and their frequency increases. The return to laminar flow over a given location is now less apt to occur. Finally, when the boundary layer is fully turbulent, high frequency, small amplitude eddies appear throughout. The small wedge heat transfer probe seems to verify this picture of the breakdown mechanism. Figure 4 shows typical oscilloscope traces from this probe for a local Mach number of approximately 9.6. The $y/\delta \simeq 0.12$ position is particularly interesting. After 1.3 msec from the beginning of the sweep, the laminar trace looks quite smooth with time. By increasing the reflected pressure P_5 the Re was increased until transition occurred. This transition trace shows a small burst at 1.5 msec followed by a return to laminar flow. At 2.1 msec a large jump in the trace is seen, indicating the passage of a large burst. A similar burst occurs at 2.7 msec. The trace then quiets down and resembles the laminar case. The turbulent trace at $y/\delta \simeq 0.12$ indicates that the flow is composed of many high-frequency, low-amplitude eddies.

The surface heat transfer oscilloscope traces (Fig. 5) show the same characteristics as the traces from the boundary-layer probe. However, the occurrence of bursts in the transition regime and the occurrence of small amplitude higher frequency eddies in the turbulent regime are not so distinct. This is probably due to the existence of a laminar sublayer.

B. Surface Heat Transfer

The local heat transfer rates on the cone surface with smooth and rough-sharp tips are presented in Figs. 6–8. The

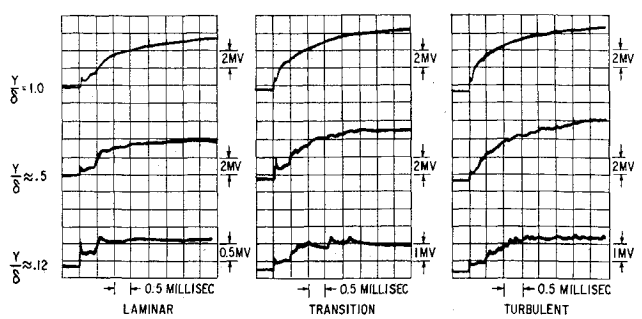

Fig. 4 Typical wedge heat transfer traces at various heights in the boundary layer at 34.5 in. from cone tip.

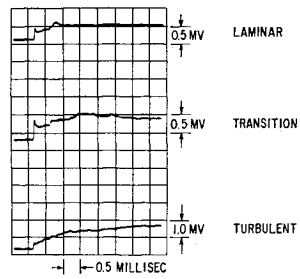

Fig. 5 Typical surface heat transfer traces for laminar, transition and turbulent flow.

laminar heat transfer theory was calculated by the method presented in Ref. 29 and using the Mangler transformation and the local Re; whereas the turbulent heat transfer rates were obtained from the theory of Li-Nagamatsu.[30] The compressibility mixing length parameter β, which accounts for the contribution of density fluctuations to the turbulent shear, was taken to be 0 and 1. For a value of unity, the contributions of the density and velocity fluctuations to this shear stress are of the same order as seen in Eq. 1:

$$\tau_w = \{[\beta\bar{u}(d\bar{\rho}/dy)] + \rho d\bar{u}/dy\} l^2 \, d\bar{u}/dy \qquad (1)$$

The skin-friction coefficients were converted to surface heat transfer rates by the modified Reynolds analogy:

$$C_h = C_f/2\sigma^{2/3} \qquad (2)$$

where σ is taken as 0.72 and the local heat transfer rate q is given by

$$q = \rho_1 u_1 C_h (H_0 - H_w) \qquad (3)$$

No transverse curvature corrections were made to this turbulent theory.

In Fig. 6, P_5 is 585 psia with a Re_x range of 2.4 to 3.8 $\times$ 10^6. These heat transfer rates had very little scatter and agreed reasonably well with the laminar theory, indicating that the boundary layer was laminar. As P_5 was increased to 1245 psia, Fig. 7, the experimental data falls above the laminar theory. An increase in the magnitude of fluctuations is also present which would indicate the passage of turbulent bursts in the transition region. Re_x for the transition case varied from 5.0 to 8.0 $\times$ 10^6.

Turbulent flow was generated in two ways. The first was to repeat the 1245 psia reservoir conditions while using the rough sharp tip instead of the smooth sharp one, Fig. 7. The second was to use the smooth sharp tip at an increased reservoir pressure of 2150 psia, Fig. 8. For $P_5 = 2150$ psia, Re_x varied from 9.7 to 14 $\times$ 10^6. The surface heat transfer distributions are shown in Figs. 7 and 8. In both figures, the experimental data is bounded by the turbulent theory for $0 \leq$

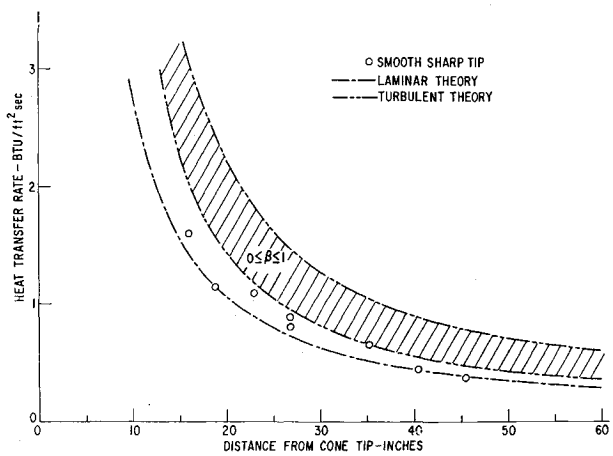

Fig. 6 Heat transfer distribution for smooth sharp cone tip at reservoir pressure $P_5 \approx 585$ psia and temperature $T_5 \approx 1400°K$.

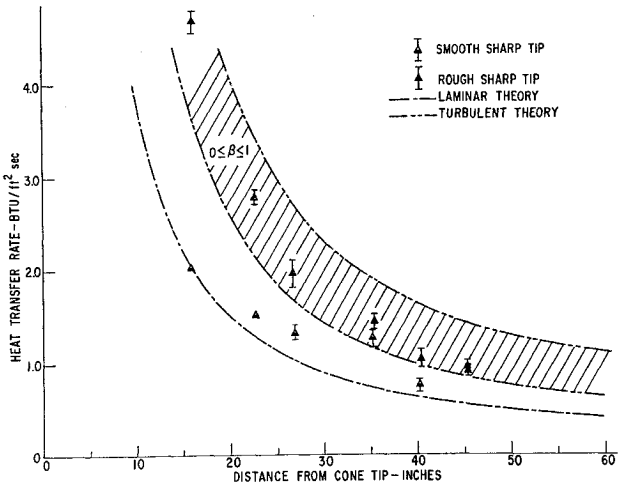

Fig. 7 Heat transfer distribution for various cone tips at reservoir pressure $P_5 \approx 1245$ and temperature $T_5 \approx 1400°K$.

$\beta \leq 1$. It will be seen later in this paper that the turbulent boundary layer generated by surface roughness had, within the experimental accuracy, the same profile as that generated by increased Re.

C. Boundary-Layer Surveys

In order to further verify the existence of various types of boundary layers, it was necessary to perform total pressure, total temperature, and wedge heat transfer surveys. These results were obtained at 34.5 in. from the cone tip where the local Mach number was 9.6. Nondimensional forms of the pitot-tube survey, P'_{o_4}/P'_{o_1}, are presented in Fig. 9. Two features are evident from the figure. The first is the much larger P'_{o_4}/P'_{o_1} gradient of the laminar curve, especially between y/δ values of 0.2 and 0.7. This had been demonstrated theoretically[31,32] and observed experimentally[2-5,33,34] at hypersonic Mach numbers. The second feature of Fig. 9 is that the turbulent boundary layer generated by tip roughness at $P_5 = 1245$ psia has essentially the same profile as that generated by the smooth sharp tip at $P_5 = 2150$ psia.

Since the cone wall was not insulated, the enthalpy could not be assumed constant across the boundary layer. This enthalpy distribution was obtained by the use of a calibrated thick film stagnation-point heat transfer probe[4] or total temperature probe. The results are shown in Fig. 9. Again the turbulent boundary layer due to either forced or natural transition appears to have the same profile. At values of y/δ

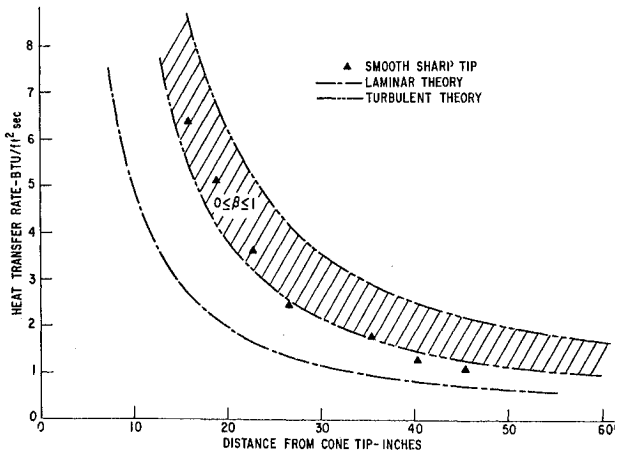

Fig. 8 Heat transfer distribution for smooth sharp cone tip at reservoir pressure $P_5 \approx 2150$ psia and temperature $T_5 \approx 1400°K$.

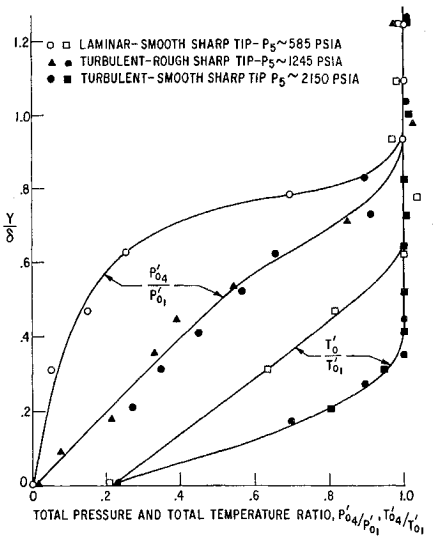

Fig. 9 Nondimensional total pressure and total temperature profiles for laminar and turbulent boundary layers, $T_5 \approx 1400°K$, $M_1 \approx 9.6$.

from 0 to 0.6 the gas flow in the turbulent boundary layer has more energy than that in the laminar boundary layer. This appears reasonable since turbulent flow is composed of eddy type motion which provides a means of transferring energy to the gas near the wall.

The nondimensional impact pressure and total temperature profiles for the transition boundary layer are presented in Fig. 10. These profiles have approximately the same shape as the turbulent profiles, indicating that the boundary layer is well into transition. However, the large fluctuation in the experimental data of Fig. 10 indicates that a fully turbulent boundary layer has not yet developed. Because to the large fluctuations in the transition boundary layer, the data curves in Figs. 10, 13, and 14 are shown as dashed lines.

Using these experimental impact pressure and total temperature distributions through the boundary layer, the velocity, density, and temperature distributions were calculated for laminar, transition and turbulent boundary layers, Figs. 11–13. For the laminar boundary layer with the smooth sharp tip, the Re, at a distance of 34.5 in. from the cone tip was 3.3×10^6 for a Mach number of 9.6. Because to a large viscous dissipation at hypersonic Mach numbers, there is a large density gradient at the outer part of this laminar boundary layer.

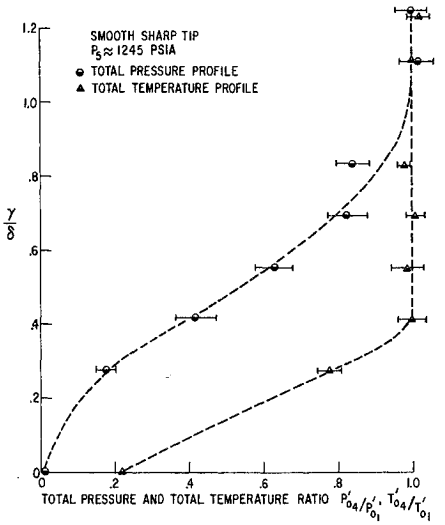

Fig. 10 Nondimensional impact pressure and impact temperature profiles for transition boundary layer, $T_5 \approx 1400°K$, $M_1 \approx 9.6$.

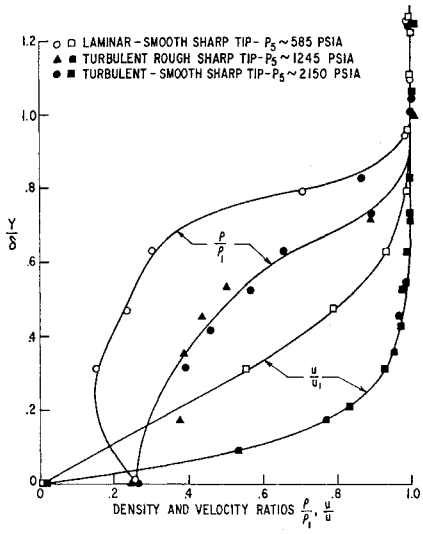

Fig. 11 Nondimensional laminar and turbulent boundary-layer profiles, $T_5 \approx 1400°K$, $M_1 \approx 9.6$.

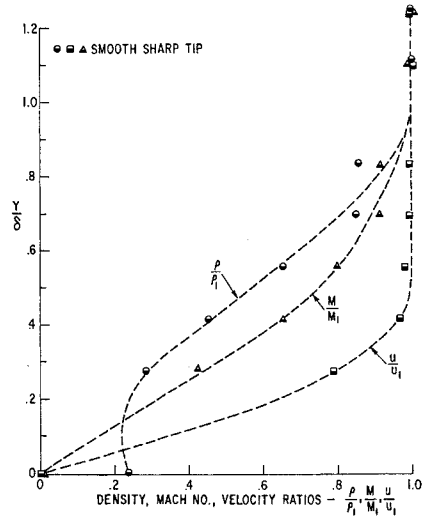

Fig. 13 Nondimensional transition boundary-layer profiles, $P_5 \approx 1245$ psia, $T_5 \approx 1400°K$, $M_1 \approx 9.6$.

Also, the density of the boundary layer near the cone surface was much less than the freestream value. Near the wall, the velocity variation is approximately linear with the vertical distance.

For the turbulent boundary layer produced by the rough sharp tip, and the transition boundary layer produced by the smooth sharp tip, the Re was 7.1×10^6. At the same location, the Re for the turbulent boundary layer produced by the smooth sharp tip is 12.2×10^6. Approximately 80% of the turbulent boundary layer is moving subsonic relative to the free stream velocity.

The heat transfer profiles in the boundary layer were determined by using two different size wedge probes.[4] In Fig. 14, the heat transfer rates for both probes in the same laminar boundary layer are presented. The small wedge probe shows higher heat transfer rates, but the sputtered platinum was located closer to the leading edge of the small wedge, giving the higher values. These measured local heat transfer rates for the small wedge were compared with the strong interaction theory of Li-Nagamatsu[35] for Mach numbers ≥ 4.5 and the flat plate theory[29] for Mach numbers ≤ 4.5. The theoretical curve was calculated by using the aforementioned theories in which the distance from the leading edge was taken to be slightly downstream from the front of the sputtered platinum gage. The agreement between the experimental and the analytical values is reasonable, considering the fact that both theories were derived on the basis of uniform flow ahead of the flat plate. Also, the results indicate that the calculated values for the conditions in the boundary layer from the measured impact pressures and total temperatures are fairly accurate. Both probes indicated the presence of flow fluctuations in the laminar boundary layer with the maximum oscillations occurring towards the outer edge as shown in Figs. 4 and 14. The heat transfer rates for the transition boundary layer in Fig. 14 show a large fluctuation throughout. A strong burst is quite evident at $y = 0.06$ in.

The heat transfer measurements for the wedge probes were made nondimensional by using the heat transfer rate just outside the boundary layer, and the results for laminar and turbulent boundary layers are presented in Fig. 15. There is a very large difference between the types of boundary layer, which was also observed at higher Mach numbers in Refs. 4 and 5. Thus, this wedge probe can be used at hypersonic Mach numbers in place of the hot wire to distinguish between laminar, transition, and turbulent boundary layers and also in obtaining the nondimensional heat transfer distribution through the boundary layer.

Figure 4 shows typical wedge heat transfer oscilloscope traces at various heights in the different boundary layers

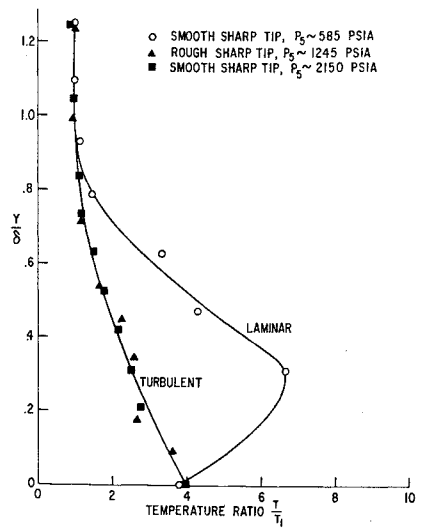

Fig. 12 Nondimensional temperature profiles for laminar and turbulent boundary layers, $T_5 \approx 1400°K$, $M_1 \approx 9.6$.

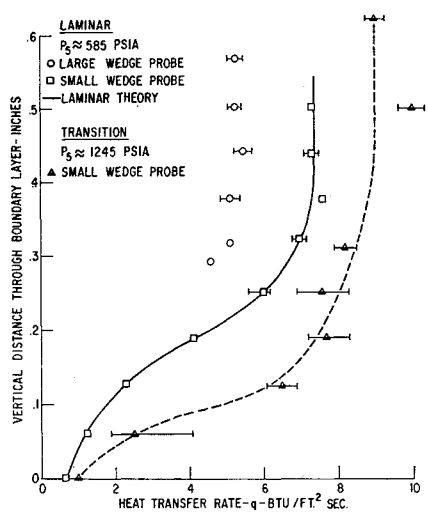

Fig. 14 Wedge probe surface heat transfer variation through laminar and transition boundary layers, $T_5 \approx 1400°K$, $M_1 \approx 9.6$.

Table 1 Displacement and momentum thickness, momentum *Re*, and heat transfer coefficient for laminar, transition, and turbulent boundary layers at $M = 9.6$

	Laminar	Transition	Turbulent	Turbulent
P_5	585 psia	1245 psia	1245 psia	2150 psia
x	34.5 in.	34.5 in.	34.5 in.	34.5 in.
$Re_{x_{\text{Int}}}$	3.35×10^6	7.1×10^6	7.1×10^6	12.2×10^6
$Re_{x_{\text{Loc}}}$	1.51×10^6	3.16×10^6	3.16×10^6	5.41×10^6
δ	0.4 in.	0.45 in.	0.7 in.	0.75 in.
δ^*	0.264 in.	0.208 in.	0.271 in.	0.291 in.
θ	6.86×10^{-4} ft	7.56×10^{-4} ft	11.12×10^{-4} ft	11.9×10^{-4} ft
Re_{δ^*}	10,700	21,460	27,430	50,610
Re_θ	334	933	1351	2490
C_h	7.32^{-4}	6.18^{-4}	7.28^{-4}	5.44^{-4}

The surveys were made at 34.5 in. from the cone tip where the local Mach number was 9.6. The differences between the laminar, transition, and turbulent traces were discussed earlier. Towards the outer edge of the boundary layer the sharp oscillations in the traces diminish until at $y/\delta = 1.0$, the laminar, transition, and turbulent traces have nearly the same characteristics. The smooth traces at $y/\delta = 1.0$ show that the freestream is probably free of large upstream disturbances.

The values of velocity and density were used to calculate the displacement thickness,

$$\delta^* = \int_0^\delta \left(1 - \frac{\rho u}{\rho_1 u_1}\right) dy \tag{4}$$

and the momentum thickness,

$$\theta = \int_0^\delta \frac{\rho u}{\rho_1 u_1}\left(1 - \frac{u}{u_1}\right) dy \tag{5}$$

When combined with freestream density, velocity, and viscosity, the momentum thickness gave the following values for momentum *Re*: laminar $Re_\theta = 334$, turbulent $Re_\theta = 1351$ for $P_5 = 1250$ psia, turbulent $Re_\theta = 2490$ for $P_5 = 2150$ psia. Values of momentum thickness, displacement thickness, momentum *Re*, heat transfer coefficient, and other quantities for laminar, transition, and turbulent boundary layers are given in Table 1.

V. Conclusions

In the transition region, the hypersonic laminar boundary layer broke down with the appearance of turbulent bursts similar to those observed at subsonic and supersonic speeds. These bursts were best detected by the small boundary layer wedge probe at $y/\delta \simeq 0.12$. The turbulent flow was characterized by high-frequency low-amplitude eddy type motion. These characteristic distinctions between laminar, transition, and turbulent flow were not so easily detected by the surface heat transfer gages.

The experimental laminar surface heat transfer rates agreed reasonably well with the laminar theory. In the transition region, there were larger fluctuations in the heat transfer rates and the mean values were higher than the laminar theory. The theoretical turbulent surface heat transfer rates for $0 \leq \beta \leq 1$ bounded the turbulent experimental results.

Boundary-layer surveys of total pressure, total temperature, and wedge probe heat transfer rates were performed at 34.5 in. from the cone tip where the local Mach number was 9.6. There was a large difference in the impact distribution between the laminar and turbulent boundary layers. From the total pressure and temperature surveys, it was possible to obtain velocity, density, temperature, and Mach number profiles. For both natural and artifically induced turbulent boundary layers, these profiles were almost identical. The magnitude of the wedge probe heat transfer rates was dependent upon the distance of the sputtered platinum gage from the leading edge of the probe. Therefore, this probe was primarily used to distinguish between the laminar, transition and turbulent boundary layers and to obtain the ratio of heat transfer rate in the boundary layer to that just outside the layer.

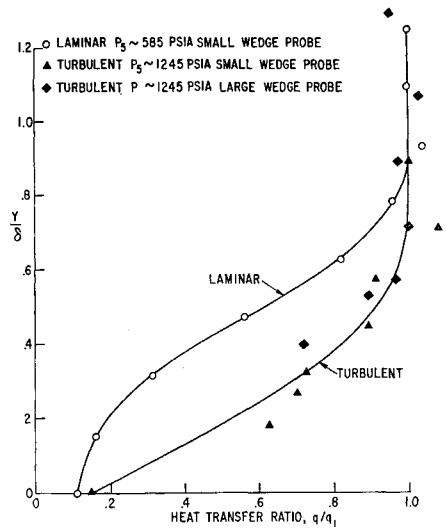

Fig. 15 Nondimensional heat transfer profiles for various types of boundary layers, $T_5 \approx 1400°K$, $M_1 \approx 9.6$.

References

[1] Nagamatsu, H. T. and Sheer, R. E., Jr., "Boundary Layer Transition on a 10° Cone in Hypersonic Flows," *AIAA Journal*, Vol. 3, No. 11, Nov. 1965, pp. 2054–2061.

[2] Nagamatsu, H. T., Graber, B. C., and Sheer, R. E., Jr., "Transition of Hypersonic Boundary Layer," *The Physics of Fluids*, Vol. 8, No. 2, Feb. 1965, pp. 211–221.

[3] Nagamatsu, H. T., Graber, B. C., and Sheer, R. E., Jr., "Roughness, Bluntness, and Angle of Attack Effects on Hypersonic Boundary Layer Transition," *Journal of Fluid Mechanics*, Vol. 24, Pt. 1, Jan. 1966, pp. 1–31.

[4] Nagamatsu, H. T., Graber, B. C., and Sheer, R. E., Jr., "Hypersonic Laminar Boundary Layer Transition on 8-Foot Long 10° Cone," *AIAA Journal*, Vol. 5, No. 7, July 1967, pp. 1245–1252.

[5] Nagamatsu, H. T., Sheer, R. E., Jr., and Wisler, D. C., "Wall Cooling Effects on Hypersonic Boundary Layer Transition, $M_1 = 7.5 - 15$," 68-C-324, Aug. 1968, General Electric Research and Development Center, Schenectady, N. Y.

[6] Nagamatsu, H. T., Wisler, D. C., and Sheer, R. E., Jr., "Hypersonic Laminar and Turbulent Skin Friction and Heat Transfer on a Slender Cone," 69-C-098, Feb. 1969, General Electric Research and Development Center, Schenectady, N. Y.

[7] Schubauer, G. B. and Klebanoff, P. S., "Contributions on the Mechanics of Boundary Layer Transition," TN 3489, 1955, NACA.

[8] Emmons, H. W., "The Laminar-Turbulent Transition in a Boundary Layer," *Journal of the Aeronautical Sciences*, Vol. 18, No. 7, July 1951, pp. 490–498.

[9] Knapp, C. F., Roache, P. J., and Mueller, T. J., "A Combined Visual and Hot-Wire Anemometer Investigation of Boundary Layer Transition," UNDAS-TR-866CK, Aug. 1966, Univ. of Notre Dame, Notre Dame, Ind.

[10] Jedlicka, J. R., Wilkins, M. E., and Seiff, A., "Experimental Determination of Boundary-Layer Transition on a Body of Revolution at M = 3.5," TN 3342, 1954, NACA.

[11] James, C. S., "Observations of Turbulent-Burst Geometry and Growth in Supersonic Flow," TN 4235, 1958, NACA.

[12] Potter, J. L. and Whitfield, J. D., "Effects of Slight Nose Bluntness and Roughness on Boundary Layer Transition in Supersonic Flows," *Journal of Fluid Mechanics*, Vol. 12, Pt. 4, 1962, pp. 508–535.

[13] Nagamatsu, H. T., Graber, B. C., and Sheer, R. E., Jr., "Critical Layer Concept Relative to Hypersonic Boundary Layer Stability," 66-C-192, June 1966, General Electric Research and Development Center, Schenectady, N. Y.

[14] Lees, L. and Reshotko, E., "Stability of the Compressible Laminar Boundary Layer," *Journal of Fluid Mechanics*, Vol. 12, Pt. 4, 1962, pp. 555–590.

[15] Laufer, J. and Verbalovich, T., "Stability and Transition of a Supersonic Boundary Layer," *Journal of Fluid Mechanics*, Vol. 9, Pt. 2, Oct. 1960, pp. 257–299.

[16] Demetriades, A., "An Experimental Investigation of the Stability of the Hypersonic Laminar Boundary Layer," *Journal of the Aeronautical Sciences*, Vol. 25, No. 9, Sept. 1958, pp. 579–600.

[17] Benney, D. J. and Lin, C. C., "On the Secondary Motion Induced by Oscillations in a Shear Flow," *The Physics of Fluids*, Vol. 3, No. 4, July 1960, p. 656.

[18] Benney, D. J., "A Non-Linear Theory for Oscillations in a Parallel Flow," *Journal of Fluid Mechanics*, Vol. 10, Pt. 2, March 1961, pp. 209–236.

[19] Klebanoff, P. S., Tidstrom, K. D., and Sargent, L. M., "The Three-Dimensional Nature of Boundary Layer Instability," *Journal of Fluid Mechanics*, Vol. 12, Pt. 1, Jan. 1962, pp. 1–34.

[20] Lin, C. C., *The Theory of Hydrodynamic Stability*, Cambridge University Press, Cambridge, England, 1955.

[21] Schlichting, H., *Boundary Layer Theory*, McGraw-Hill, New York, 1960.

[22] Lees, L. and Lin, C. C., "Investigation of the Stability of the Laminar Boundary Layer in a Compressible Fluid," TN 1115, 1946, NACA.

[23] Lees, L., "The Stability of the Laminar Boundary Layer in a Compressible Fluid," TR 876, 1947, NACA.

[24] Lees, L. and Reshotko, E., "Stability of the Compressible Laminar Boundary Layer," *Journal of Fluid Mechanics*, Vol. 12, Pt. 4, 1962, pp. 550–590.

[25] Nagamatsu, H. T., Geiger, R. E., and Sheer, R. E., Jr., "Hypersonic Shock Tunnel," *ARS Journal*, Vol. 29, 1959, pp. 332–340.

[26] Nagamatsu, H. T., Weil, J. A., and Sheer, R. E., Jr., "Heat Transfer to Flat Plate in High Temperature Rarefied Ultrahigh Mach Number Flow," *ARS Journal*, Vol. 32, 1962, pp. 533–541.

[27] "Mollier Diagram for Equilibrium Air," March 1964, ARO Inc., Arnold Air Force Station, Tenn.

[28] Weil, H., "Effects of Pressure Gradient on Stability and Skin Friction in Laminar Boundary Layers in Compressible Fluids," *Journal of the Aeronautical Sciences*, Vol. 18, No. 5, May 1951, pp. 311–318.

[29] Howarth, L., "*Modern Developments in Fluid Dynamics High Speed Flow*," Vol. 1, Oxford University Press, London, 1953, p. 402.

[30] Li, T. Y. and Nagamatsu, H. T., "Effect of Density Fluctuations on the Turbulent Skin Friction on a Flat Plate at High Supersonic Speeds," GALCIT No. 11, Nov. 1952, California Institute of Technology, Pasadena, Calif.

[31] Von Kármán, T. and Tsien, H. S., "Boundary Layer in Compressible Fluids," *Journal of the Aeronautical Sciences*, Vol. 6, No. 5, May 1938, pp. 227–232.

[32] Van Driest, E. R., "Investigation of the Laminar Boundary Layer in Compressible Fluids Using the Crocco Method," AL-1183, Jan. 1951, North American Aviation Inc., Englewood, Calif.

[33] Kendall, J. M., Jr., "An Experimental Investigation of Leading Edge Shock Wave Boundary Layer Interaction at Mach 5.8," *Journal of the Aeronautical Sciences*, Vol. 24, No. 1, 1957, pp. 47–56.

[34] Korkegi, R., "Transition Studies and Skin Friction Measurements on an Insulated Flat Plate at a Mach Number of 5.8," *Journal of the Aeronautical Sciences*, Vol. 23, No. 1, 1956, pp. 97–107.

[35] Li, T. Y. and Nagamatsu, H. T., "Hypersonic Viscous Flow on a Non-Insulated Flat Plate," *Proceedings of the 4th Midwestern Conference on Fluid Mechanics*, Purdue University, No. 128, 1955, pp. 273–287.

MARCH 1971 J. AIRCRAFT VOL. 8, NO. 3

Minimum Time Turns for a Supersonic Airplane at Constant Altitude

J. KARL HEDRICK* AND ARTHUR E. BRYSON JR.†
Stanford University, Stanford, Calif.

Optimal control theory is used to determine thrust, bank-angle, and angle-of-attack programs for minimum time turns of a supersonic airplane at constant altitude for three different terminal conditions: 1) both heading angle and velocity specified, 2) only heading angle specified, 3) only velocity specified. The angle-of-attack is constrained to be less than the stall angle of the aircraft and the thrust is constrained to be less than the maximum attainable thrust, which at constant altitude is a function of velocity. Numerical results are given for a typical supersonic airplane at two different altitudes. These results show that in general a variable velocity, variable bank angle turn at full throttle is minimizing.

Nomenclature

C_{D_0} = zero lift drag coefficient
$C_{L\alpha}$ = lift coefficient curve slope ($dC_L/d\alpha$)
D = drag
D_L = drag due to lift
D_0 = zero lift drag
g = acceleration of gravity
H = Hamiltonian
L = lift
L_α = lift curve slope ($dL/d\alpha$)
m = mass of aircraft
M = Mach number
q = dynamic pressure
S = area
T = thrust
T_M = maximum thrust
V = velocity
W = weight
α = angle-of-attack
α_s = angle-of-attack at stall
β = heading angle
η = aerodynamic efficiency factor
σ = bank angle
λ_v = velocity adjoint
λ_β = heading angle adjoint
μ_1 = thrust constraint adjoint
μ_2 = angle-of-attack constraint adjoint
ρ = density of atmosphere

* Research Assistant, Department of Aeronautics and Astronautics; now Assistant Professor of Mechanical Engineering, Arizona State University.

† Professor of Applied Mechanics, Aeronautics and Astronautics. Fellow AIAA.